Very High Resolution SAR Speckle and CCD

Daniel Andre and Keith Morrison
Centre for Electronic Warfare, CDS,
The Defence Academy of the United Kingdom,
Cranfield University,
Shrivenham, UK
e-mail: d.andre@cranfield.ac.uk

David Blacknell, Darren Muff, Matthew Nottingham and Claire Stevenson
Defence Science and Technology Laboratory,
Porton Down, Salisbury, UK

***Abstract*—Synthetic Aperture Radar (SAR) Coherent Change Detection (CCD) has been found to be of great utility in detecting changes that occur on the ground. Detectable changes of interest include vehicle tracks, water flow, and small scale subsidence. The CCD procedure involves performing repeat pass radar collections to form a coherence product, where ground disturbances can induce detectable incoherence. Currently, SAR imagery of between 10cm and 30cm resolution is considered to be a high resolution, allowing the detection of subtle changes on the ground, however it is of interest to examine SAR image speckle characteristics and corresponding CCD images resulting from very high resolution SAR down to 1cm resolution, which in principle could be collected through airborne or spaceborne radar platforms. To perform this study, laboratory data was generated with a ground-based SAR system.**

Keywords — Radar; SAR; speckle; CCD; coherent change detection; UWB

I. INTRODUCTION

Synthetic Aperture Radar (SAR) Coherent Change Detection (CCD) has been found to be of great utility in detecting changes that occur on the ground. Detectable changes of interest include vehicle tracks, water flow, and small scale subsidence. The CCD procedure involves performing repeat pass radar collections to form a coherence product, where ground disturbances can induce detectable incoherence [1]-[5].

Currently, SAR imagery of between 10cm and 30cm resolution is considered to be a high resolution, allowing the detection of subtle changes on the ground, however it is of interest to examine CCD images resulting from very high resolution SAR down to 1cm resolution, which in principle could be collected through airborne or spaceborne radar platforms [6]. To perform this study, laboratory data was generated with the Cranfield University Ground-Based SAR system (GB-SAR) [7][8].

The laboratory SAR system is first described, and the requirements for SAR imagery of different resolution are presented. Pyramidal antenna horns, nominally calibrated for X-band 8-12GHz were employed in this study, and first results within this band are presented. However for the 15GHz bandwidth collection, calibration proved difficult, so a filtering process was employed instead, resulting in the very high resolution SAR and CCD images presented.

II. GB-SAR MEASUREMENTS

The GB-SAR system is a portable stepped frequency CW imaging radar which has been employed both indoors and outdoors [7][8]. For the experiments reported here, the system was deployed indoors at a laboratory within Cranfield University, UK, as seen in Fig.1. The antenna horn was mounted on a SAR rail 1.60m above the floor and incrementally stepped across different imaging apertures, up to 3.50m wide, with a predefined step size interval. A band between 5GHz and 20GHz was employed, thus providing up to 15GHz bandwidth. The slant range to scene center was approximately 3.75m, so that the 2.4m x 3.6m rectangular gravel scene was effectively imaged in the SAR near-field. Monostatic SAR measurements were conducted by attaching the receiver horn to the moving rail, however bistatic and multistatic SAR and CCD measurements can also be conducted with the system [4]. A calibration was conducted for the X-band pyramidal horns between 8GHz and 12GHz, providing initial results of resolution down to 4cm. Metal spheres of diameter 3cm and 5cm were arranged to either side of the gravel scene to allow for image alignment and resolution estimation. The changes made to the gravel to evaluate the level of CCD were implemented by gently moving a stick over the gravel. The gravel stones were nominally 1cm in diameter.

Figure 1. The GB-SAR system set up indoors with a gravel scene to be imaged. The X-band antenna horns are mounted on a SAR rail, which is mounted on the Green “Niftylift120” trailer. Metal spheres, with both 3cm and 5cm diameter are setup on either side (left and right) to aid in image alignment and resolution estimation.

Throughout, image formation was performed with the SAR back-projection algorithm, which is suitable for the SAR near-field scenario [1].

III. RESOLUTION

Because the scene center is only 3.75m from the SAR rail, and the aperture length can be as much as 3.5m wide, the scene is in the SAR near-field. This has the effect that different points within the scene can have different radar azimuth angle apertures as well as radar grazing / elevation angles, which in its turn implies that the SAR image resolution is spatially variant. Additionally, the point spread function will be irregular and will also vary in form from place to place. The resolution quoted in the following however, is always that estimated at the scene centre. It is noted that in principle the back-projection imaging algorithm can be modified to compensate for the spatial variation in resolution [4][5], however this was not implemented for this study. It would be difficult to compensate for the variation in the form of the point spread function however.

The ground range resolution is given by [1]

$$r_r = \frac{c}{2B\cos(e)} \quad (1)$$

Where c is the speed of light, B is the frequency bandwidth employed, and e is the radar grazing angle, evaluated as 27.3°. The cross range resolution is given by [1]

$$r_{cr} = \frac{c}{2f_c 2\sin(\theta/2)\cos(e)} \quad (2)$$

Where f_c is the centre frequency transmitted, and θ is the azimuth angle aperture, given by

$$\theta = 2\ \mathrm{atan}\left(\frac{L_{\mathrm{ap}}}{2R}\right) \quad (3)$$

Where L_{ap} is the azimuth SAR aperture length and R is the closest range to scene center.

With a minimum frequency of 5GHz and maximum aperture length of 3.5m, for a given bandwidth B, the centre frequency is given by

$$f_c = \frac{5 + (B+5)}{2} \quad (4)$$

Hence one may plot SAR resolution as a function of frequency bandwidth, as shown in Fig.2, where the solid curve is the range resolution and the dashed curve is the cross-range resolution. In the figure it can be seen that as the bandwidth increases, the range and cross-range resolution curves improve, coming closer together and eventually crossing in the bandwidth region between 12GHz and 15GHz where a resolution just over 1cm is achieved.

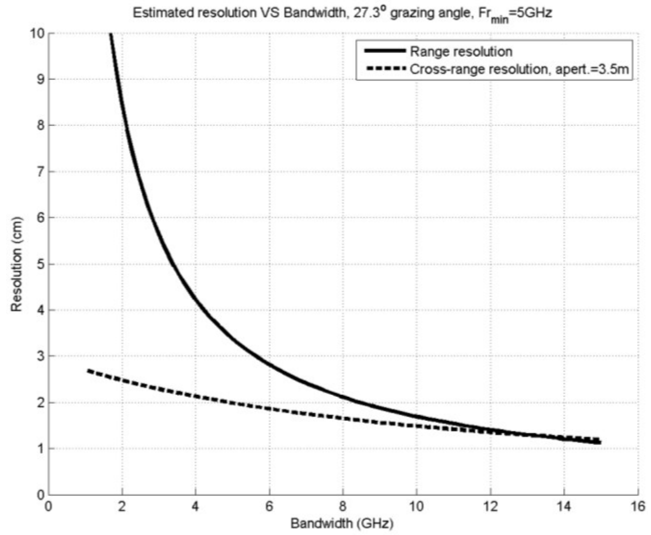

Figure 2. Graph showing range and cross-range SAR resolution as a function of frequency bandwidth, with minimum frequency set at 5GHz. Range resolution is given by the solid black curve and cross-range resolution, for the 3.5m aperture length is given by the dashed curve. The finest resolution achievable is just over 1cm.

IV. HIGH RESOLUTION SAR SPECKLE AND CCD

Initial high resolution SAR images were formed within the calibration range of the pyramidal horns. The X-band calibration frequency range was from 8GHz to 12GHz, allowing a maximal bandwidth of 4GHz.

Generally, SAR resolutions within the range of 30cm to 10cm are already considered to be of high resolution [1]. However a bandwidth of 4GHz allows resolutions down to 4.2cm. For comparison with later *very high resolution* images, in this section SAR image and speckle characteristics results are presented for 10cm resolution in Fig.3 and 4.2cm resolution in Fig.4. In both cases, SAR aperture length is set so that the cross-range resolution matches the range resolution.

Verifying that the SAR images satisfy theoretical predictions for speckle would indicate that the SAR system and near-field geometry employed allow a well-controlled CCD experiment to be undertaken. The theoretical intensity probability distribution for speckle is given by

$$P(I) = \frac{1}{\langle I \rangle}\exp\left(\frac{-I}{\langle I \rangle}\right) \quad (5)$$

where I is the intensity and $\langle I \rangle$ is the mean intensity [1].

In order to measure the SAR intensity distribution at a given nominal resolution, a central portion of the various SAR images was extracted. This is necessary because SAR resolution is spatially variant in the SAR near-field geometry. Then for easier cross comparison of results across the SAR image extracts, pixel intensity was normalized by division by the mean intensity. The resulting intensity histograms were also normalized for easier cross comparison – the normalization was by total pixel number, and the bin widths were normalized due to varying maximum pixel intensity.

 ISBN: 978-1-61208-397-1

For 10cm SAR resolution, the full SAR images, the SAR image extracts and the corresponding normalized intensity histogram plots are shown in Fig.3(a), (b) and (c) respectively. The theoretical speckle distribution is shown as the red curve overlaid on the histogram plot. The corresponding plots for 4.2cm SAR resolution are shown in Fig.4(a), (b) and (c) respectively.

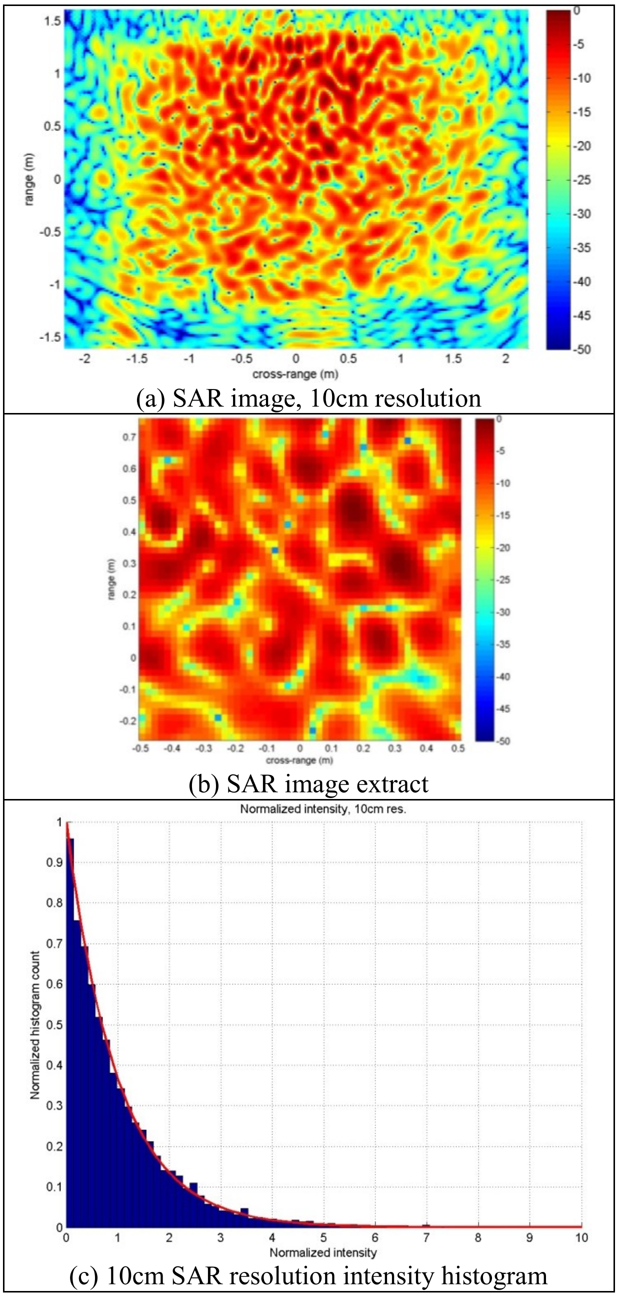

(a) SAR image, 10cm resolution

(b) SAR image extract

(c) 10cm SAR resolution intensity histogram

Figure 3. SAR image (a), approximately **10cm resolution**, of gravel scene with metal spheres arranged on left and right. The frequency bandwidth is **1.7GHz (10GHz centre frequency)**; (b) extract from center of SAR image for speckle analysis, (c) normalised intensity histogram overlaid by the theoretical speckle intensity probability distribution.

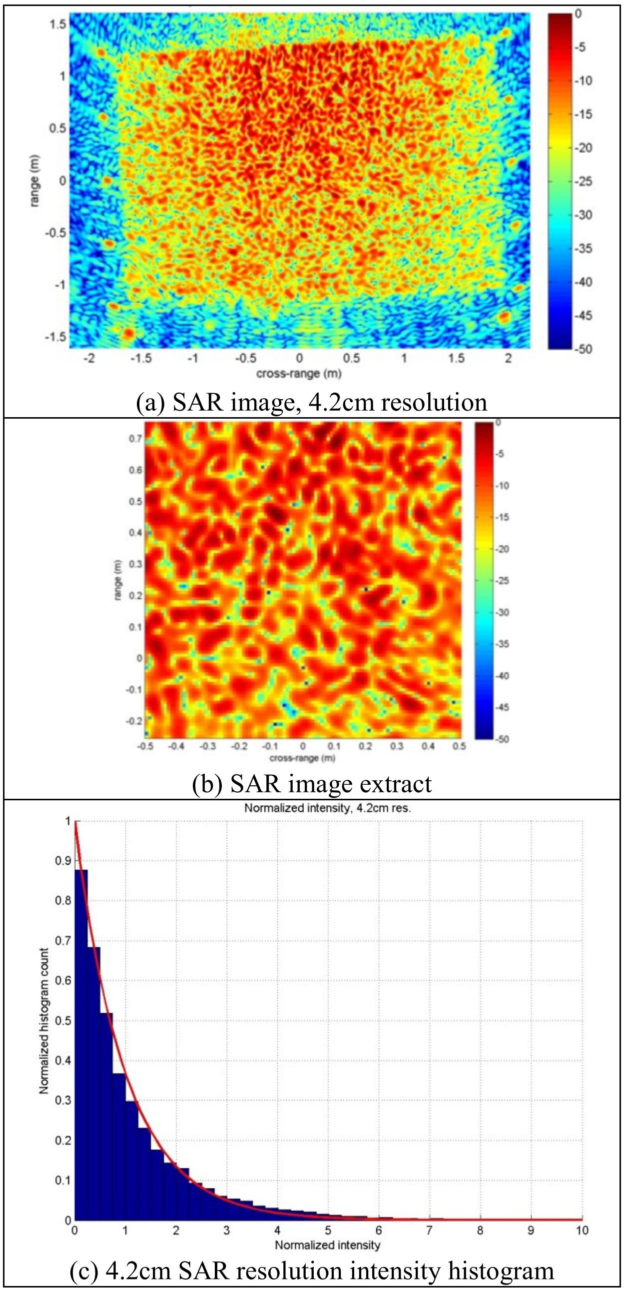

(a) SAR image, 4.2cm resolution

(b) SAR image extract

(c) 4.2cm SAR resolution intensity histogram

Figure 4. SAR image (a), approximately **4.2cm resolution**, of gravel scene scene with metal spheres arranged on left and right. The frequency bandwidth is **4GHz (8-12GHz)**; (b) extract from center of SAR image for speckle analysis, (c) normalized intensity histogram overlaid by the theoretical speckle intensity probability distribution.

For both resolutions, it can be seen that the histogram bar charts follow the theoretical curves very closely, indicating that the SAR images have well developed speckle characteristics, which will allow for a controlled CCD experiment.

Light disturbances were made to the gravel scene by gently scraping a stick over the gravel, allowing the formation of CCD products. The 10cm and 4.2cm SAR image resolution CCD products are shown in Fig.5(a) and (b) respectively.

The disturbances were neither evident directly to the eye, nor evident in the corresponding individual SAR images, but they are evident in the CCD images of Fig.5. However, the exact nature of the disturbances is difficult to determine at these resolutions (they should spell out some words).

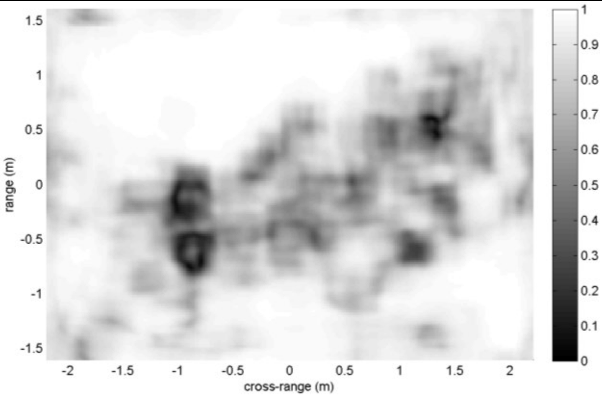

(a) 10cm resolution SAR image CCD

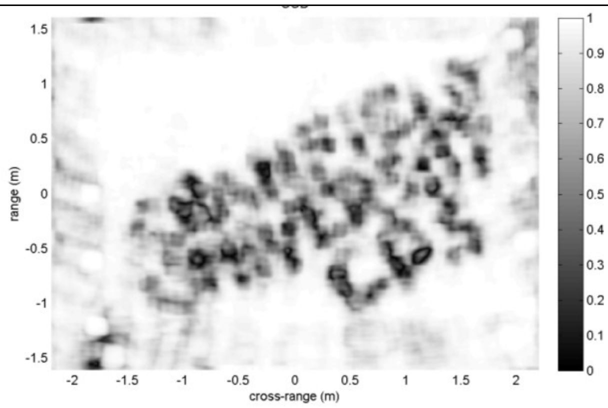

(b) 4.2cm resolution SAR image CCD

Figure 5. CCD images showing some disturbance to the gravel. One of the 10cm resolution SAR images used to form CCD a) can be seen in Fig.3(a). One of the 4.2cm resolution SAR images used to form CCD b) can be seen in Fig.4(a).

V. VERY HIGH RESOLUTION SAR AND CCD

In section IV, SAR and CCD images formed within the calibrated range of the antenna horns were presented. There, a bandwidth of 4GHz was employed, achieving a resolution down to 4.2cm. The system however, is capable of larger bandwidths up to 15GHz, potentially achieving very high range resolution down to 1cm, as can be predicted in Fig.2. Additionally the full aperture length of 3.5m can be employed, which will also potentially achieve very high cross-range resolution down to 1cm at these frequencies, as predicted in Fig.2.

For the purposes of the evaluation of SAR and CCD quality at very high resolutions and given the stable behavior of pyramidal horns over wide bandwidths, it was determined that it would likely be sufficient to employ signal processing filters, instead of a full calibration, which proved difficult over the full 15GHz bandwidth range.

The raw pulse amplitudes in the frequency domain are presented in Fig.6(a). It can be seen that there is a very large variation in amplitude in the recorded signal, which cannot be due to the scene. Hence for the purposes of SAR image formation, two successive filters were employed, resulting in a cleaner and more uniform amplitude signal in the frequency domain, where some underlying scene structure is made visible, as seen in Fig.6(b).

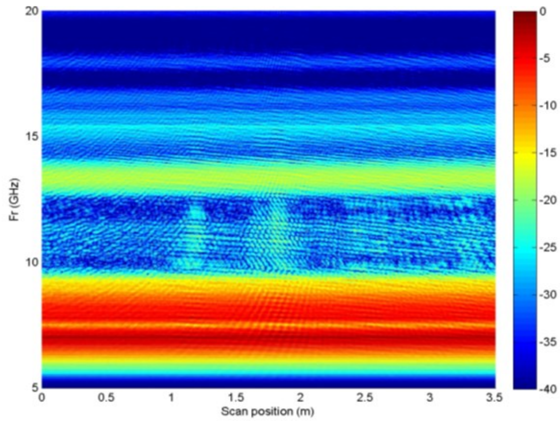

(a) Frequency domain, raw scan data

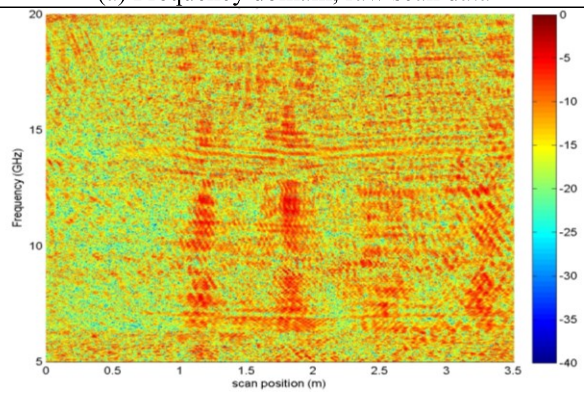

(b) Frequency domain, filtered scan data

Figure 6. raw frequency domain scan data (a) (frequency VS scan position on rail), showing large variation in recorded intensity; (b) filtered frequency domain scan data.

The two successive filters are as follows:

1. The first is the subtraction of system noise: The average complex pulse signal is determined over all of the pulses and is then subtracted from the raw dataset;
2. The second filter to be employed is a normalization filter: The mean absolute pulse is determined and divided through all of the pulses, thus normalizing the overall amplitude, whilst leaving the underlying structure in the data

After having filtered the raw data (from the state in Fig.6(a) to that in Fig.6(b), image formation is performed, providing SAR images such as that seen in Fig.7(a). A close inspection of features within the image confirms that a resolution of approximately 1cm has been obtained: Examination of the metal sphere signatures supports this, as well as examination of the speckle structure over the gravel scene in the SAR image extract in Fig.7(b), which should be of the same size as the image resolution [1].

The normalized intensity histogram for the SAR image extract, shown in Fig.7(c), shows very close agreement with the theoretical intensity distribution for speckle shown as the overlaid red curve.

The corresponding CCD image shown in Fig.8 can be seen to be of high quality, and now at the very high SAR resolution the nature of the disturbance is clearly evident, and can be seen to spell out “Cranfield University CDS”.

The additional disturbance evident on the bottom left of the CCD image is mostly outside of the gravel area, and was found to be due to a change in the articulation of a window at the far end of the laboratory. The window was open during the reference image collection, producing some sidelobes in that region, but it had been closed during the second SAR scan, so that the sidelobes were absent. The result thus became apparent in the CCD product.

VI. CONCLUSION

This work has examined very high resolution SAR images down to 1cm resolution, and corresponding CCD images, collected in a laboratory environment by a ground-based SAR system. The SAR image intensity distributions closely matched theoretical intensity probability distributions for speckle.

The resulting CCD images showed subtle change detections to a scale that was not possible with conventional high resolution SAR images of resolution down to 10cm.

In principle, these techniques can be applied to remote sensing at these very fine resolutions if desired.

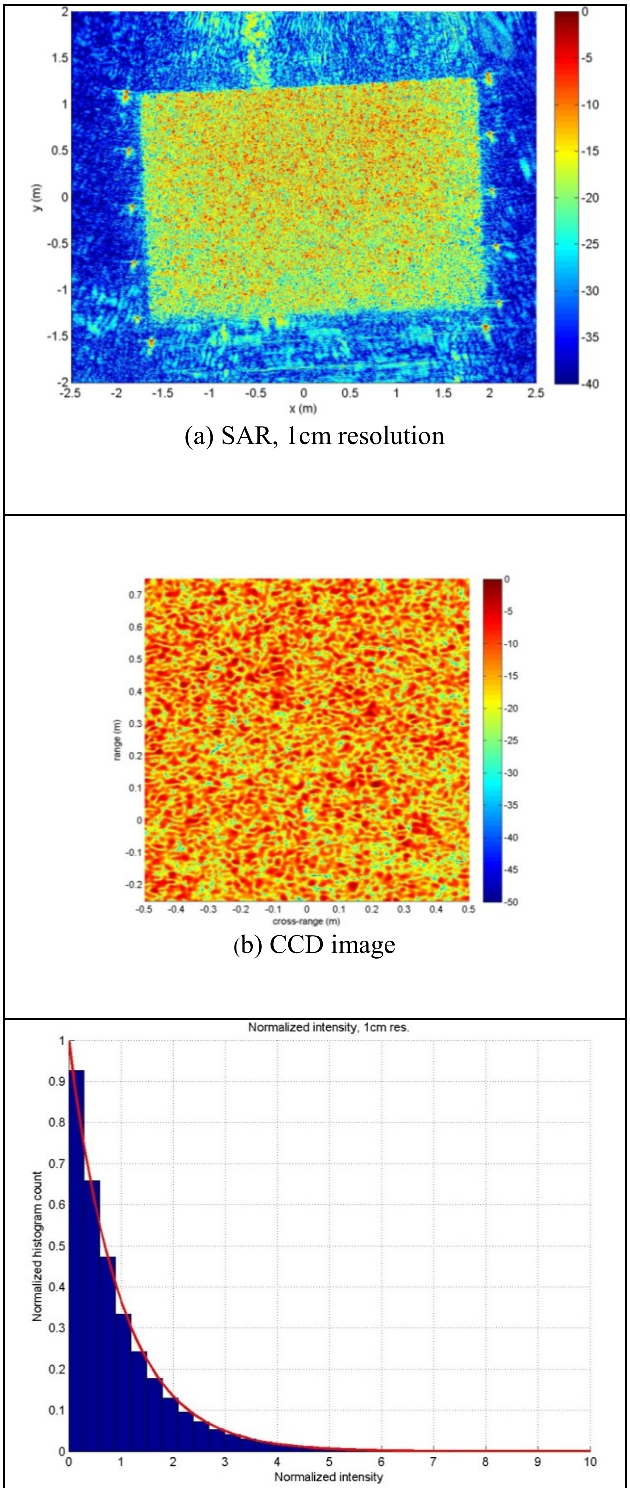

(a) SAR, 1cm resolution

(b) CCD image

(c) 1cm resolution intensity histogram

Figure 7. SAR image, approximately **1cm resolution**, of gravel scene with metal spheres arranged on left and right (a). The frequency bandwidth is **15GHz (5-20GHz)**, and the SAR rail aperture is **3.5m**; (b) extract from center of SAR image for speckle analysis, (c) normalised intensity histogram overlaid by the theoretical speckle intensity probability distribution.

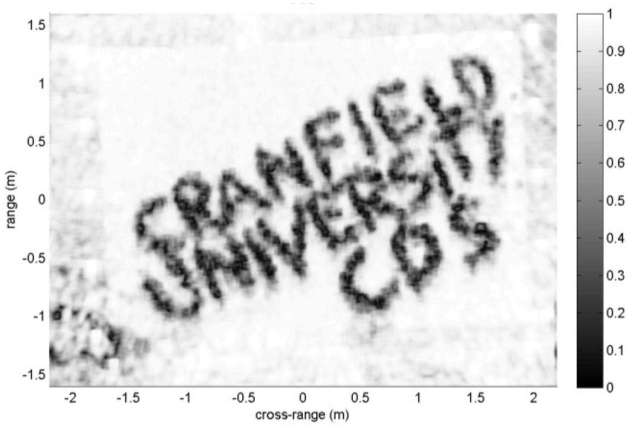

Figure 8. CCD image showing the disturbance to the gravel, spelling out "Cranfield University CDS". One of the 1cm resolution SAR images used to form this CCD can be seen in Fig.7(a).

ACKNOWLEDGMENT

This work was funded by the Defence Science and Technology Laboratory, UK.

REFERENCES

[1] C. V. Jakowatz Jr., D. E. Wahl, P. H. Eichel, D. C. Ghiglia, P. A. Thompson, "Spotlight-Mode Synthetic Aperture Radar: A Signal Processing Approach", Kluwer Academic Publishers, 1999.

[2] M. Preiss and N. J. S. Stacy, "Coherent Change Detection: Theoretical Description and Experimental Results", Technical Report, Defence Science and Technology Office, Australia, DSTO-TR-1851, August 2006.

[3] D. Blacknell, D. B. Andre and C. M. Finch, "SAR coherent change detection (CCD) over mountainous regions", International conference on synthetic aperture sonar and synthetic aperture radar (SAS/SAR), 13th-14th September 2010.

[4] D. B. André, D. Blacknell and K. Morrison, "Spatially variant incoherence trimming for improved SAR CCD", SPIE DSS 2013, April 2013.

[5] D. B. André, D. Blacknell. and K. Morrison, "Spatially variant incoherence trimming for improved bistatic SAR CCD", IEEE Radar Conference 2013, 1st -5th April 2013.

[6] D. G. Muff, D. Blacknell and M. R. Nottingham, "Pharos – a SAR concept to accelerate advanced exploitation", IET International Conference on Radar Systems, October 2012.

[7] K. Morrison, J. C. Bennett, G. Cookmartin, A. J. McDonald, A. Race and S. Quegan "Three-dimensional X-band SAR imaging of a small conifer tree", Int. J. Remote Sens., 22, p705 (2001).

[8] S. C. M. Brown, S. Quegan, K. Morrison, J. C. Bennett and G. Cookmartin, "High resolution measurements of scattering in wheat canopies – implications for crop retrieval." IEEE Transactions of Geoscience and Remote Sensing, 41, p1602-1610 (2003).